

Fusion-excitation-function analyses with a dynamic model

M. Blann and D. Akers

E. Division, Lawrence Livermore National Laboratory, Livermore, California 94550

(Received 26 March 1982)

Sixteen heavy ion induced fusion excitation functions are analyzed using Swiatecki's new dynamic model. The systems selected span a target-projectile range between $^{12}\text{C} + ^{14}\text{N}$ to $^{86}\text{Kr} + ^{209}\text{Bi}$. The effective threshold and extra energy parameters were held at the values deduced by Swiatecki from ^{208}Pb induced reactions, in order to display systematic scaling behavior with target and projectile mass and angular momentum. Agreement between experimental results and model predictions seem excellent for most systems investigated. A tendency to go from a rolling to sliding friction mode is noted as one goes to lighter systems. There is also some indication that the threshold parameter may decrease for lighter systems.

[NUCLEAR REACTIONS Heavy ion fusion excitation functions, compared with predictions of new dynamic fusion model of Swiatecki.]

I. INTRODUCTION

Fusion excitation functions are generally characterized by a region which gives a linear relationship when plotted versus $\epsilon_{c.m.}^{-1}$. This region has been used to deduce values of internuclear potentials at an effective fusion radius, as well as the value of the radius.¹⁻⁴

Beyond some energy, this linear σ_{fusion} vs ϵ^{-1} relationship ceases to describe the data. Early attempts to describe this aspect of the fusion excitation functions involved one dimensional potential models consisting of the Coulomb, nuclear, and centrifugal potentials for the two approaching ions, both assumed to remain spherical.⁵⁻⁷ The question of fusion was related to the existence or disappearance of a relative minimum or "pocket" in the one dimensional potential. Modifications involving a dissipative parameter have also been introduced into such analyses. An informative review article has been written for analyses of this type.⁸

A new and different approach to the question has appeared, a new dynamic reaction model due to Swiatecki.^{9,10} The new model has been formulated as a schematic model intended to use the minimum degrees of freedom and simple inertial treatments in order to illustrate the mechanisms expected in binary collision processes, in a model permitting closed form solutions of many of the relevant equations of motion.

The new model differs from the "pocket" models in several very basic aspects. One of these is that a conditional saddle point is defined which considers the entrance channel asymmetry, but which also

contains a neck degree of freedom. (Analyses of fusion excitation functions have indicated the importance of a neck in that fusion radii are consistent with substantial surface overlap between the interacting nuclei.) Secondly, the question of fusion is given a geometric and dynamic treatment in the new approach, as opposed to the question of the existence of a pocket in a one dimensional potential. Specifically, the question is raised as to whether the contact configuration of the interacting ions lies inside or outside the conditional saddle shape; i.e., the compactness of the contact configuration is compared with the compactness of the conditional saddle point.

Many different reaction mechanisms may be described by different trajectories which are globally described in this new dynamic model. In the present work analyses are performed with respect to one model prediction, that of a required "extra push" for fusion when the contact configuration is less compact than the conditional saddle point configuration. (The extra push is an additional radial injection energy to push the contact configuration to a shape which is more compact than a conditional saddle shape.) This results in deviations of the predicted fusion excitation functions from the linear relationship versus ϵ^{-1} , and these deviations may be compared with experimental results.

We will present results of analyses of fusion excitation functions for systems from $^{12}\text{C} + ^{14}\text{N}$ to $^{86}\text{Kr} + ^{209}\text{Bi}$ in order to probe for mass dependent deviations of the formulation from the data. Results of this type should be helpful in guiding more precise calculations, which we understand are in

progress.¹¹ The new dynamic reaction model should have far reaching consequences in interpreting many phenomena which have been observed, but not yet adequately understood in heavy ion reactions. Some of these will be discussed in Sec. IV.

In Sec. II, a brief description of the new model as it pertains to the prediction of fusion excitation functions is presented. Comparisons with data comprise Sec. III. Discussions and conclusions comprise Sec. IV.

II. FUSION EXCITATION FUNCTIONS AND THE NEW DYNAMIC MODEL

Reaction paths are first determined by a conditional saddle point in the mode under discussion. If the contact configuration lies inside the conditional saddle, then there is no inhibition to fusion. The fusion excitation function may then be described by the usual semiclassical formulation

$$\sigma(\epsilon) = \pi R^2 (1 - V_{\text{fus}}/\epsilon), \quad (1)$$

where ϵ is the center of mass energy, and R and V_{fus} the radii and potential energies at the contact radii, respectively.

The conditional saddle point is defined for the frozen target-projectile mass asymmetry of the entrance channel (which nonetheless includes some degree of neck formation). The location of the conditional saddle point is made (for headon collisions) using Bass's parameter,⁶

$$(Z^2/A)_{\text{eff}} = 4Z_1 Z_2 / [A_1^{1/3} A_2^{1/3} (A_1^{1/3} + A_2^{1/3})], \quad (2)$$

where A_1, A_2, Z_1, Z_2 represents target and projectile mass and charge. This disruptive parameter may be seen to represent the ratio of Coulomb disruptive to surface attractive forces. It reduces to Z^2/A , the familiar fissility parameter, for symmetric systems.

In order to scale the conditional saddle point value for angular momentum, a first order correction was suggested by Swiatecki by which the ratio of centrifugal to surface forces is added to (2),

$$(Z^2/A)_{\text{eff tot}} = (Z^2/A)_{\text{eff}} + (L/L_{\text{ch}})^2 \quad (3)$$

where L is the angular momentum and

$$L_{\text{ch}} = \frac{emr_0}{2f} \frac{A_1^{2/3} A_2^{2/3} (A_1^{1/3} + A_2^{1/3})}{A_1 + A_2}. \quad (4)$$

In (4), e is the unit of charge, m the nucleon mass

(931 MeV/c²), r_0 the nuclear constant, and f the fraction of the total angular momentum responsible for the radial centrifugal force. For rolling motion of two spheres, $f = \frac{5}{7}$; for sliding motion, $f = 1$; and for rigidly sticking spheres,

$$f^{-1} = 1 + \frac{2}{5} \frac{(1 + A_2/A_1)}{A_2/A_1} \times \frac{[1 + (A_2/A_1)^{5/3}]}{[1 + (A_2/A_1)^{1/3}]^2}. \quad (5)$$

The model predicts that an extra radial injection energy ΔE is required to push the contact configuration inside the conditional saddle when it is outside. The contact shape is predicted to lie outside the conditional saddle point shape when the value $(Z^2 A)_{\text{eff tot}}$ of (3) exceeds some critical threshold value. The value 33 ± 1 has been deduced as a value for the critical threshold by fitting a set of fusion excitation functions for reactions of ²⁰⁸Pb ions with targets from ²⁴Mg (Refs. 10 and 12) to ⁶⁴Ni. The value found empirically may be justified from "first principles."¹⁰

The form predicted for the extra injection energy is given by Swiatecki as

$$\Delta E = 0, \quad [(Z^2/A)_{\text{eff tot}} \leq (Z^2/A)_{\text{eff thr}} \approx 33], \quad (6a)$$

$$\Delta E = K [(Z^2/A)_{\text{eff tot}} - (Z^2/A)_{\text{eff thr}}]^2, \quad \text{if } (Z^2/A)_{\text{eff tot}} \geq 33, \quad (6b)$$

where

$$K = \frac{A_1^{1/3} A_2^{1/3} (A_1^{1/3} + A_2^{1/3})^2}{A_1 + A_2} \times \frac{32}{2025} \left[\frac{3}{\pi} \right]^{2/3} \left[\frac{e^2}{\hbar c} \right]^2 mc^2 a^2. \quad (7)$$

The constant a is to be determined either empirically or from theoretical considerations. We will use the value $a = 12$ deduced empirically in Ref. 10.

Swiatecki has provided a closed form equation for the fusion cross section when (6b) applies,

$$\sigma(E) = \frac{\pi R^2}{E} \left\{ \left[\left[\frac{C_1 C_2 + \frac{1}{2}}{C_2^2} \right]^2 - \frac{C_1^2 + V_B - \epsilon}{C_2^2} \right]^{1/2} - \frac{C_1 C_2 + \frac{1}{2}}{C_2^2} \right\}, \quad (8)$$

where

$$C_1 = \sqrt{K} \left[(Z^2/A)_{\text{eff tot}} - (Z^2/A)_{\text{eff thr}} \right] \quad (9)$$

and

$$C_2 = \frac{\sqrt{K}}{e^2 r_0} \frac{8f^2}{A_1^{1/3} A_2^{1/3}} \quad (10)$$

We have used Eq. (8) in evaluating experimentally measured evaporation residue and/or fusion excitation functions. Values of f corresponding to sliding, rolling, and sticking motion have been used in three sets of calculations, with the values of $a = 12$ and $(Z^2/A)_{\text{eff thr}} = 33$. Where good fusion data existed which were adequately described by Eq. (1), values of R and V_B were taken from slope and intercept analyses of $\sigma(\epsilon)$ vs ϵ^{-1} ; otherwise the parametrizations of Vaz, Alexander, and Satchler were used.¹³ These comparisons with data are presented in Sec. III.

III. COMPARISONS OF CALCULATED AND EXPERIMENTAL FUSION EXCITATION FUNCTIONS

Fusion is defined within Swiatecki's model as reactions for which the dynamic path has passed inside the conditional saddle point. This would include reactions yielding evaporation residue products and fissionlike products. In principle, parts of either type of cross section may result from paths which do not pass inside the true (compound nucleus) saddle point. Deep inelastic reactions should in principle be excluded from the fission cross section. Clearly an ambiguity may exist in unfolding experimentally measured cross sections; this ambiguity increases as target-projectile asymmetry decreases. It will be noted for some of the data sets presented.

The comparisons of Eq. (8) with various data sets are presented in Figs. 1–8. Most experimental excitation functions are shown with energy (c.m.) as abscissa; however, some are versus ϵ^{-1} . The data were measured by many different groups. The review paper of Birkelund *et al.*⁸ was used as the source for the data presented in Figs. 1, 6, 7, and 8. The original data sources are referenced in the figure captions.^{1–4, 14–34}

In all figures the results of the semiclassical Eq. (1) are shown by a solid curve. In Fig. 1 for Kr induced reactions of Ho and Bi nuclei it may be seen that the upper limit points are consistent with the extra push predictions of Eq. (8). We note that for

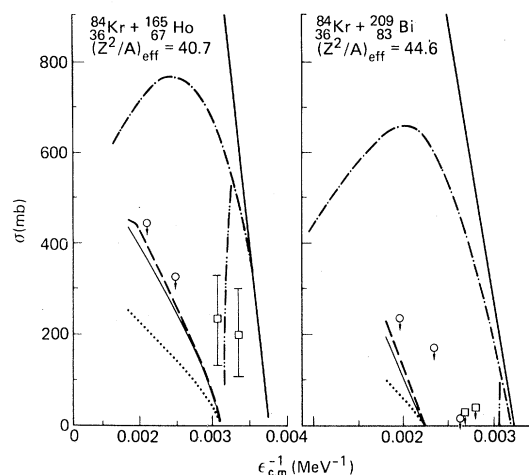


FIG. 1. Fusion limits deduced from fissionlike yield measurements for ^{84}Kr induced reactions of ^{165}Ho and ^{209}Bi ; data are from Refs. 14 and 15. The heavy solid line represents predictions of the semiclassical formula Eq. (1). The dashed, thin solid, and dotted curves beginning on the abscissa represent predictions of Eq. (8) with values of f corresponding to sticking, rolling, and sliding motion, respectively. The dashed-dotted and dashed-dotted-dotted curves are predictions of one dimensional pocket models as reported in Ref. 8. The values of $(Z^2/A)_{\text{eff}}$ due to Coulomb contributions alone are indicated in the figure. Arrows on data points represent upper limits to cross sections.

such heavy systems, the $(Z^2/A)_{\text{eff}}$ of Eq. (2) exceeds the critical threshold values. For results presented in Figs. 2–8, the centrifugal contributions to Eq. (3) are required before $(Z^2/A)_{\text{eff total}}$ of Eq. (3)

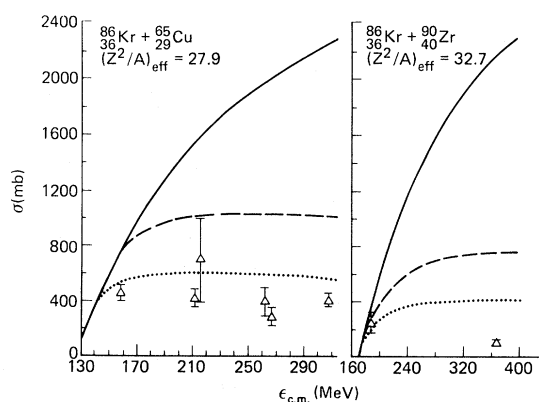


FIG. 2. Evaporation residue excitation functions for ^{86}Kr induced reactions of ^{65}Cu and ^{90}Zr . The solid curve is the fusion prediction of Eq. (1). The dashed and dotted curves represent predictions for fusion with f for sticking and sliding motion, respectively. The rolling limit is indistinguishable from the sticking limit for these systems due to the near symmetry of the entrance channels. Experimental results are from Refs. 16 and 17.

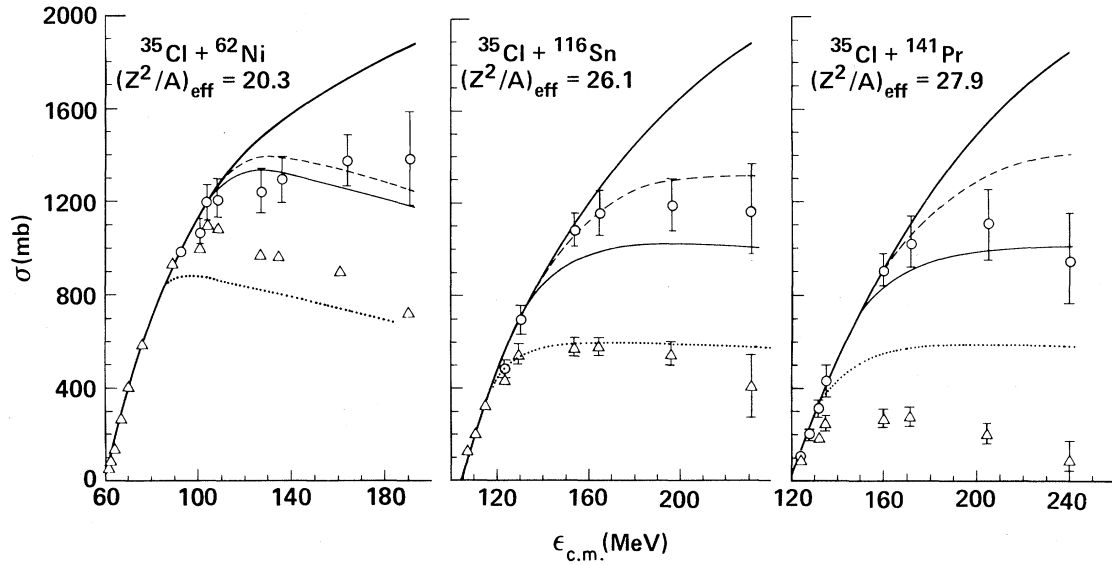


FIG. 3. Fusion excitation functions for ^{35}Cl induced reactions of ^{62}Ni , ^{116}Sn , and ^{141}Pr . Data are from Refs. 1, 2, 4, and 18. Triangles represent evaporation residue cross sections. Circles represent the sum of fissionlike plus evaporation residue cross sections. Contamination of deep-inelastic products is probable for the $^{35}\text{Cl} + ^{62}\text{Ni}$ system. Calculated results are as in Fig. 2; the thin solid curve represents Eq. (8) with the rolling motion value for f .

exceeds the critical threshold value of 33. [The $(Z^2/A)_{\text{eff}}$ values are indicated in each figure.]

A larger set of heavy system data was presented in Ref. 12, for which the excitation function shapes predicted by Eq. (8) have excellent agreement with the data. It may be seen in Fig. 1, as was shown more clearly in Ref. 12, that the one dimensional pocket model predictions are inconsistent with ex-

perimental results for very heavy systems.

In Fig. 2 comparisons are made between Eq. (8) and experimental evaporation residue cross sections. Since the fissionlike component is ambiguous for these systems due to the near symmetry in the entrance channels, only the lower limits to the fusion cross sections can be compared.

A better data set is shown in Fig. 3. Of the three systems shown, the $^{62}\text{Ni} + ^{35}\text{Cl}$ data have uncertain admixtures of deep inelastic yields in the fissionlike products. For these data the fusion excitation function lies somewhere between the ER and ER + fissionlike yields. For the ^{116}Sn and ^{141}Pr targets fusion results should be represented by the sums of ER plus fissionlike yields shown. The agreement with Eq. (8) is very good for values of f between the sticking and rolling limits.

In Fig. 4, there is some question as to whether the highest energy (214 MeV ^{16}O) ER point for $^{16}\text{O} + ^{40}\text{Ca}$ is compound nucleus in nature. The fissionlike yields for this system are very small (< 100 mb) so that the ER yields should represent the fusion cross sections adequately. Yet compound nuclei should be limited by fission at a lower angular momentum than is indicated by the reported ER cross section at 214 MeV. Results for this system seem consistent with Eq. (8) with f between sliding and rolling values; the highest energy point follows a different slope than, e.g., the $^{40}\text{Ar} + ^{109}\text{Ag}$ system.

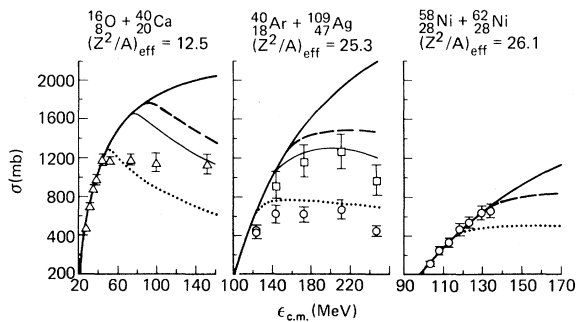


FIG. 4. Fusion excitation functions for reactions of ^{16}O , ^{40}Ar , and ^{58}Ni as indicated. For $^{16}\text{O} + ^{40}\text{Ca}$ the triangles represent evaporation residue yields in Ref. 19; very small upper limits to fission were reported. For $^{40}\text{Ar} + ^{109}\text{Ag}$ (Ref. 16) the circles are ER yields and squares are sums of ER plus an estimated unfolding of a symmetric fission contribution. Circles for $^{58}\text{Ni} + ^{62}\text{Ni}$ represent ER yields from Ref. 20; no significant fissionlike yields were reported. Calculated results are as in Figs. 2 and 3.

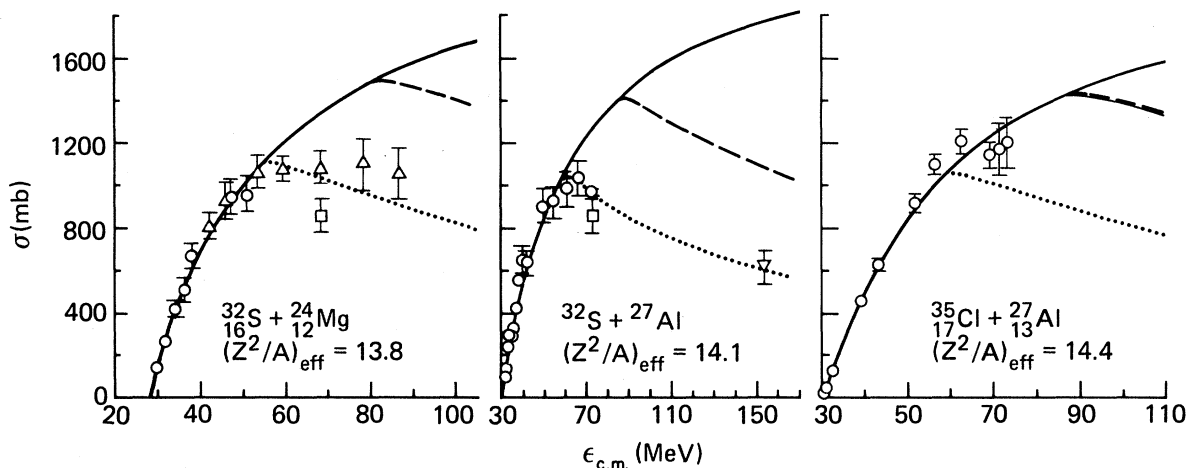


FIG. 5. Fusion excitation functions for ^{32}S and ^{35}Cl induced reactions. Data are from Refs. 3, 4, and 21–23. All data points represent ER cross sections. Calculated results are as in Figs. 2 and 3.

For the $^{40}\text{Ar} + ^{109}\text{Ag}$ system of Fig. 3, the authors attempted to unfold the fissionlike yields from the deep inelastic yields. The fusion cross sections shown should therefore be valid within the error bars shown. Equation (8) reproduces the experimental results very well using “ f ” for rolling motion. For the $^{58}\text{Ni} + ^{62}\text{Ni}$ excitation function the evaporation residue results extend high enough in

energy to show an incompatibility with Eq. (8) for sliding motion. The ER cross sections represent the fusion cross sections for this system.

In Fig. 5 the evaporation residue excitation functions are consistent with Eq. (8) for sliding motion. The question of fissionlike yields which would increase fusion cross section over ER results is open, although in general significant fissionlike yields have not been observed for such light systems.

In Fig. 6 the ER yields should represent the fusion yields. Equation (8) gives good agreement with the data when sliding motion is assumed.

In Figs. 7 and 8 the sliding motion limit is preferred, but it also appears that a critical threshold value less than 33 is required to fit the data.

IV. DISCUSSION AND CONCLUSIONS

For the heaviest systems presented, the threshold requirement for the extra push for fusion results primarily from the Coulomb contribution to the disruptive parameter of Eq. (3). For these systems the fusion excitation functions seem to be reproduced well when motion between rolling and sticking is assumed for the system at contact. Progressing to lighter systems, where the major disruptive parameter contribution to the extra push requirement comes from the centrifugal component, the data seem to be reproduced by a calculation requiring rolling motion. Finally, for the lightest system presented, $^{12}\text{C} + ^{14}\text{N}$, a lower value of $(Z^2/A)_{\text{eff}}$ may also be required.

The range of target/projectile masses covered in Figs. 1–8 is indeed impressive when considering that the model itself is schematic in nature, employ-

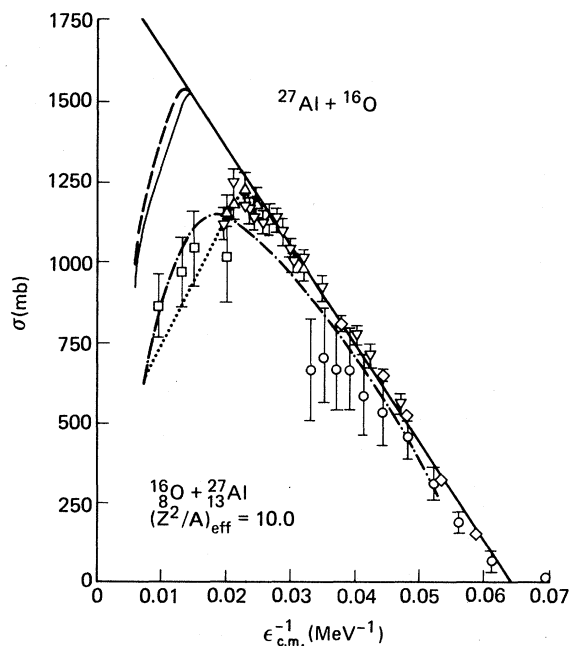


FIG. 6. Fusion excitation function for $^{16}\text{O} + ^{27}\text{Al}$. Experimental ER cross sections are from Refs. 22–26. The dashed-dotted curve is the result of a one-dimensional pocket model calculation as reported in Ref. 8. Other curves are as in Figs. 2 and 3.

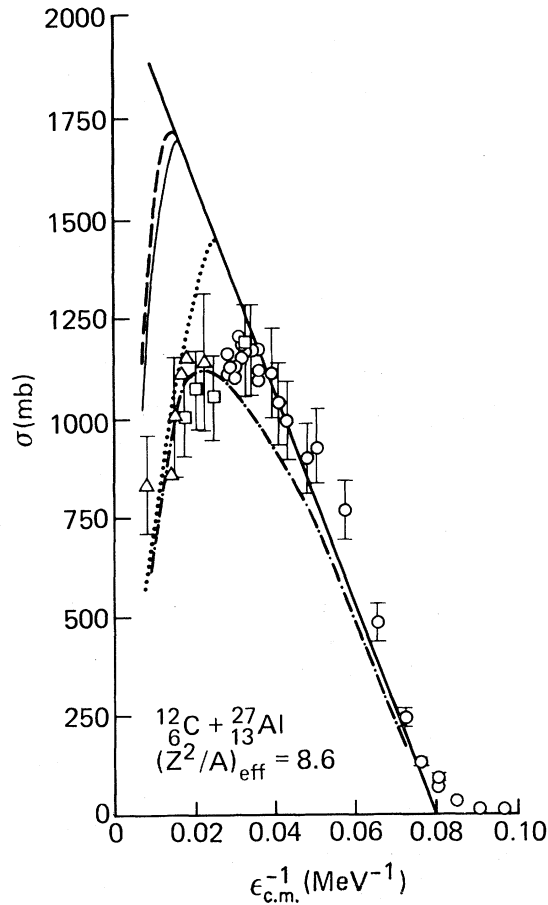


FIG. 7. Fusion excitation functions for $^{12}\text{C} + ^{27}\text{Al}$. Experimental ER cross sections are from Refs. 27–29. The dashed-dotted curve is a one dimensional pocket model result from Ref. 8. Other curves are as in Figs. 2 and 3.

ing the bare minimum in degrees of freedom and parameters which would be required to reproduce the main features of the reactions. Yet while liquid drop parametrizations with the associated sharp surfaces were used in the formulation, the data sets of Figs. 1–8 go from systems which are mostly saturation density nuclear matter, to systems where a majority of nucleons are in the surface. The disruptive parameter was used to scale systems from those for which it was mostly Coulomb, to those for which it was mostly centrifugal. For the lighter systems, the mechanism of entrance channel breakup for light heavy ions may complicate further the question of the validity of the data for testing the model.

The broad success of the new dynamic model shown in Figs. 1–8 gives strong testimony to the value of its basic underlying assumptions. This provides a great incentive to pursue the concepts

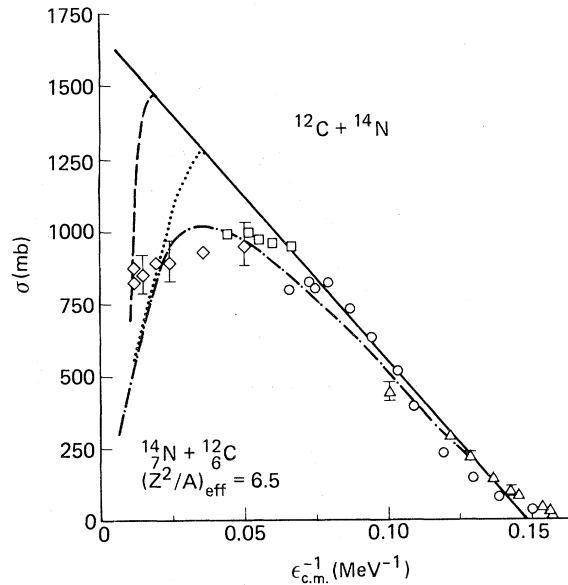


FIG. 8. Fusion excitation functions for $^{12}\text{C} + ^{14}\text{N}$. Experimental ER yields are from Refs. 30–34. Curves are as defined in Figs. 2, 3, and 7.

with calculations of a more detailed nature. We note that the first order method of scaling angular momentum effects as if they were Coulomb effects should not be valid over the broad ranges encountered in the analyses of this work; Coulomb and centrifugal effects are expected to influence saddle point shapes somewhat differently. Additionally the surface diffuseness will affect the moment of inertia and radial force components versus the sharp surface values of the present schematic model, and should lead to considerably different scaling for the light systems which exceed the fusion threshold value only at high angular momenta. It will also be these lighter systems which may show the larger changes due to finite range effects^{35,36} when more rigorous calculations are performed. Therefore interesting extensions of this model may be expected to include a more precise treatment of the angular momentum scaling. The manner in which the $(Z^2/A)_{\text{eff thr}}$ and a parameters may be expected to change with mass should also be investigated further, as has been recommended by Swiatecki.

We note that the simple pocket model prescription appears to work better for the data in Figs. 6–8 than Swiatecki's new dynamic model. Our opinion is that there is nothing to be gained by dwelling on this circumstance based on a physically incorrect and oversimplified model. This opinion is in part supported by the failure of the pocket model

to fit the high Z data, as well as by obvious physical deficiencies of this approach. We rather feel that the failure of the new dynamic model as shown in Figs. 6–8 should help to improve the model through considerations of the type discussed above.

The new dynamic model has already proven of value in suggesting “best” reactions and energies for synthesizing heavy elements. It makes several interesting predictions with respect to reaction mechanisms and barriers to fusion and compound nucleus formation. An exciting possibility for the future involves the fact that absolute time dependences are predicted for different trajectories of the reaction surface. This may permit calculations as to the spectral distributions and multiplicities of

light particles emitted between the contact configuration and passage inside the true compound saddle point. In analogy to the quasifission mechanism, we should come to appreciate quasievaporation as a dissipative mechanism in this regime. Perhaps such a mechanism will provide a key to observations not yet understood in terms of existing mechanisms. We are quite optimistic that the new dynamics will play a very broad role, and indeed provide a footing for understanding a broad range of heavy ion reaction phenomena.

The authors appreciate enlightening discussions with Dr. W. J. Swiatecki.

-
- ¹B. Sikora *et al.*, Phys. Rev. C 20, 2219 (1979).
²B. Sikora *et al.*, Phys. Rev. C 21, 614 (1980).
³H. H. Gutbrod, W. G. Winn, and M. Blann, Nucl. Phys. A213, 267 (1973).
⁴W. Scobel, H. H. Gutbrod, M. Blann, and A. Mignerey, Phys. Rev. C 14, 1808 (1976).
⁵J. Galin, D. Guerreau, M. Lefort, and X. Tarrago, Phys. Rev. C 9, 1018 (1974).
⁶R. Bass, Nucl. Phys. A231, 45 (1974).
⁷R. Bass, Phys. Rev. Lett. 39, 265 (1977).
⁸J. R. Birkelund, L. E. Tubbs, J. R. Huizenga, J. N. De, and D. Sperber, Phys. Rep. C56, 107 (1979).
⁹W. J. Swiatecki, Phys. Scr. 24, 113 (1981).
¹⁰W. J. Swiatecki, Nucl. Phys. A376, 275 (1982).
¹¹W. J. Swiatecki, private communication.
¹²H. Sann *et al.*, Phys. Rev. Lett. 47, 1248 (1981).
¹³L. C. Vaz, J. M. Alexander, and G. R. Satchler, Phys. Rep. 69, 373 (1981).
¹⁴J. Péter, C. Ngo, and B. Tamain, Nucl. Phys. A250, 351 (1975).
¹⁵K. L. Wolf *et al.* (unpublished).
¹⁶H. C. Britt *et al.*, Phys. Rev. 13, 1483 (1976).
¹⁷F. Plasil *et al.*, Phys. Rev. 18, 2603 (1978).
¹⁸B. Sikora *et al.*, Phys. Rev. C 25, 686 (1982).
¹⁹S. E. Vigdor *et al.*, Phys. Rev. C 20, 2147 (1979).
²⁰B. Sikora *et al.*, Phys. Rev. C 25, 885 (1982).
²¹D. G. Kovar, P. D. Bond, C. Flaum, M. J. Levine, and C. E. Thorn, Bull. Am. Phys. Soc. 22, 66 (1977), reported in Ref. 8.
²²R. L. Kozub *et al.*, Phys. Rev. C 11, 1497 (1975).
²³Y. Eisen, I. Tseruya, Y. Eyal, Z. Fraenkel, and M. Hillman, Nucl. Phys. A291, 459 (1977).
²⁴B. Back *et al.*, Nucl. Phys. A285, 317 (1977).
²⁵J. Dauk, K. P. Lieb, and A. M. Kleinfeld, Nucl. Phys. A241, 170 (1975).
²⁶R. Rascher, W. F. J. Muller, and K. P. Lieb, reported in Ref. 8.
²⁷R. R. Betts, W. A. Lanford, M. H. Mortensen, and R. L. White, Argonne National Laboratory Report ANL/Phys. 76-2, 1976, p. 443.
²⁸R. R. Betts, private communication quoted in Ref. 8.
²⁹J. B. Natowitz, E. T. Chulick, and M. N. Namboodiri, Phys. Rev. C 6, 2133 (1972).
³⁰R. G. Stokstad, J. Gomez del Campo, J. A. Biggerstaff, A. H. Snell, and P. H. Stelson, Phys. Rev. Lett. 36, 1529 (1976).
³¹D. G. Kovar, Proceedings of the IPCR Symposium on Macroscopic Features of Heavy Ion Collisions and Pre-equilibrium Processes, Hakone, 1977, IPCR Cyclotron Report Suppl. 6, p. 18.
³²J. A. Kuehner and E. Almquist, Phys. Rev. 134B, 1229 (1964).
³³W. Henning *et al.*, Bull. Am. Phys. Soc. 22, 629 (1977).
³⁴Z. E. Switkowski, R. G. Stokstad, and R. M. Wieland, Nucl. Phys. A279, 502 (1977).
³⁵H. G. Krappe and J. R. Nix, in *Proceedings of the Third International Atomic Energy Agency Symposium on the Physics and Chemistry of Fission, Rochester, 1973* (IAEA, Vienna, 1974), Vol. I, p. 159.
³⁶H. J. Krappe, J. R. Nix, and A. J. Sierk, Phys. Rev. 20, 992 (1979).